

# Compositional Oil Spill Detection Based on Object Detector and Adapted Segment Anything Model from SAR Images

Wenhui Wu, Man Sing Wong, Xinyu Yu, Guoqiang Shi, Coco Yin Tung Kwok, and Kang Zou

**Abstract**—Semantic segmentation-based methods have attracted extensive attention in oil spill detection from SAR images. However, the existing approaches require a large number of finely annotated segmentation samples in the training stage. To alleviate this issue, we propose a composite oil spill detection framework, SAM-OIL, comprising an object detector (e.g., YOLOv8), an adapted Segment Anything Model (SAM), and an Ordered Mask Fusion (OMF) module. SAM-OIL is the first application of the powerful SAM in oil spill detection. Specifically, the SAM-OIL strategy uses YOLOv8 to obtain the categories and bounding boxes of oil spill-related objects, then inputs bounding boxes into the adapted SAM to retrieve category-agnostic masks, and finally adopts the Ordered Mask Fusion (OMF) module to fuse the masks and categories. The adapted SAM, combining a frozen SAM with a learnable Adapter module, can enhance SAM’s ability to segment ambiguous objects. The OMF module, a parameter-free method, can effectively resolve pixel category conflicts within SAM. Experimental results demonstrate that SAM-OIL surpasses existing semantic segmentation-based oil spill detection methods, achieving mIoU of 69.52%. The results also indicated that both OMF and Adapter modules can effectively improve the accuracy in SAM-OIL.

**Index Terms**—Oil Spill Detection, Object Detection, Segment Anything Model, Adapter.

## I. INTRODUCTION

SYNTHETIC Aperture Radar (SAR) is one of the most efficient remote sensing tools for detecting oil spills [1], [2]. One challenge in oil spill detection is to distinguish between oil spills and look-alikes, as both appear as dark spots in SAR imagery. Previous studies suggested that contextual information is beneficial to oil spill detection [1], [3]. Krestenitis *et al.* [4] developed a multi-class semantic segmentation dataset, which includes oil spill, look-alike, land, ship, and sea surface. In this letter, we cite this dataset as

Manuscript received xxx, xxx; revised xxx, xxx. This work was supported in part by the General Research Fund (project ID: 15609421 and 15603920); by the Hong Kong Ph.D. Fellowship Scheme from the Research Grants Council of Hong Kong; and by the Environment and Conservation Fund under Grant 2021-107. (Corresponding author: Man Sing Wong)

M.S. Wong is with the Department of Land Surveying and Geo-Informatics, The Hong Kong Polytechnic University, Kowloon, Hong Kong, and also with the Research Institute for Sustainable Urban Development, The Hong Kong Polytechnic University, Hung Hom, Kowloon, Hong Kong (e-mail: ls.charles@polyu.edu.hk).

W. Wu, X. Yu, G. Shi, C.Y.T. Kwok, and K. Zou are with the Department of Land Surveying and Geo-Informatics, The Hong Kong Polytechnic University, Kowloon, Hong Kong (e-mail: wenhui.wu@polyu.edu.hk; 19109597r@connect.polyu.hk; guoqiang.shi@polyu.edu.hk; ytcoco.kwok@connect.polyu.hk; welly.zou@polyu.edu.hk).

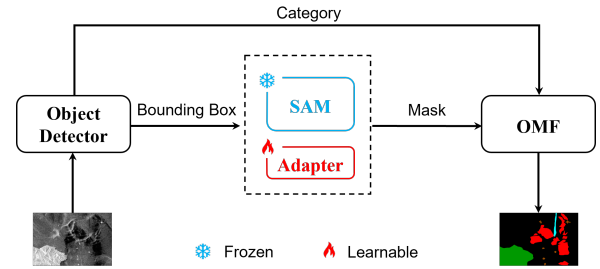


Fig. 1. Architecture of the proposed method. The Adapted SAM is composed of a frozen SAM and a learnable Adapter module. SAM-OIL consists of an object detector, an Adapted SAM, and an OMF module.

the Multimodal Data Fusion and Analytics (M4D) dataset, following the terminology of the proposing team’s institution.

The traditional approach to detect oil spills on SAR images consists of three steps: dark spot segmentation, feature extraction, and distinguishing oil spills from look-alikes [1], [2]. Firstly, dark spots on the SAR image are extracted through traditional segmentation methods. Then, various features such as geometric, contextual, texture, and physical features are extracted from these dark areas. Finally, a traditional classifier such as Support Vector Machine or Random Forest is used to distinguish oil spills from look-alikes [5]. However, the method has certain limitations, such as issues of under-segmentation or over-segmentation during the segmentation process, limited expressive capability of manually designed features, and the relatively weak discriminative ability of traditional classifiers in identifying oil spills. Therefore, there is still room for improvement in the accuracy of oil spill detection.

Deep learning-based methods have gained increasing attention in oil spill detection owing to their powerful capability in feature expression [2]. Previous studies either directly used classical semantic segmentation models to detect oil spills, or developed tailor-made adaptive semantic segmentation models based on the characteristics of oil spills for the detection [4], [6]. In addition, the integration of polarimetric features in these models further enhances detection accuracy [7], [8]. Although these methods provided reasonably good detection performance, they required accurately annotated segmentation samples for training, which is generally time-consuming and resource-intensive for building the dataset.

To alleviate the need for a large number of finely annotated

samples in semantic segmentation methods, we propose a composite oil spill detection framework, SAM-OIL, comprising an object detector (e.g., YOLOv8), an adapted Segment Anything Model (SAM), and an Ordered Mask Fusion (OMF) module. SAM represents the latest advancements in natural image segmentation, which offers impressive zero-shot segmentation performance by using input prompts such as points, bounding boxes, masks, and text [9]. Among the types of prompts, those based on bounding boxes have led to the best segmentation results [10], hence, we integrate the object detector with SAM for oil spill detection. The YOLO series models are the most efficient models in object detection, so we chose the latest YOLOv8 [11] as the object detector in the SAM-OIL framework. On the other hand, the outputs of SAM are category-agnostic binary masks, which may cause pixel category conflicts when masks are merged. To solve this issue, we proposed the Ordered Mask Fusion (OMF) module, which merges masks according to a predefined category order to improve the final accuracy. Furthermore, directly applying the SAM trained on natural images to remote sensing satellite imagery does not yield satisfactory results [10], especially for SAR images with blurred object boundaries. To bridge this gap, SAM needs to be adapted specifically for the oil spill detection tasks. HQ-SAM [12] is the minimal adaptation of SAM, which enhances the segmentation accuracy of SAM by adding less than 0.5% of model parameters. Due to the simplicity and training efficiency of HQ-SAM, we integrate the Adapter module from HQ-SAM into SAM-OIL, thereby transferring the segmentation capability of SAM to the oil spill detection task. The main contributions of this study are summarized as follows.

- We propose a compositional oil spill detection framework called SAM-OIL, which combines an advanced object detector (e.g., YOLOv8) with the SAM. To our best knowledge, this is the first time the SAM has been applied to oil spill detection.
- Ordered Mask Fusion (OMF) module is proposed, which is a parameter-free method, to effectively resolve pixel category conflicts in SAM.
- We introduce an Adapter module from HQ-SAM into the SAM-OIL, which utilizes masks from M4D dataset to train the Adapter, effectively enhancing SAM's segmentation capabilities for objects with fuzzy boundaries.
- Experimental results demonstrate that SAM-OIL achieves mIoU of 69.52%, surpassing existing oil spill detection methods, and both OMF and Adapter can effectively improve the accuracy of SAM-OIL.

The rest of this letter is organized as follows. Section II describes the methods proposed. Section III performs a series of quantitative and qualitative analyses via experiments. Section IV concludes this letter.

## II. METHODOLOGY

The architecture of the proposed method is given in Fig. 1. SAM-OIL consists of an object detector (i.e., YOLOv8), an Adapted SAM, and an OMF module. We refer to the combination of YOLOv8 and frozen SAM as YOLOv8-SAM, which is considered as the baseline of our method.

### A. YOLOv8-SAM

SAM consists of three components: an image encoder  $\Phi_{enc-i}$ , a prompt encoder  $\Phi_{enc-p}$ , and a lightweight mask decoder  $\Phi_{dec-m}$ . SAM takes an image  $I$  and a set of prompts  $P$  as inputs, which first uses  $\Phi_{enc-i}$  to obtain image features  $F_I$ , and encodes the prompts  $P$  into sparse prompt tokens  $T_P$  through  $\Phi_{enc-p}$ . Then,  $T_P$  and some learnable output tokens  $T_O$  are concatenated, and finally input into  $\Phi_{dec-m}$  along with  $F_I$  for attention-based feature interaction, generating category-agnostic binary masks  $M$ . This process can be described as:

$$\begin{cases} F_I &= \Phi_{enc-i}(I) \\ T_P &= \Phi_{enc-p}(P) \\ M &= \Phi_{dec-m}(F_I, \text{Concat}(T_O, T_P)) \end{cases} \quad (1)$$

YOLOv8-SAM is composed of an object detector and a frozen SAM. The procedure is as follows: 1) The object detector  $\Phi_{det}$  obtains the object categories  $C_{bbox}$ , bounding boxes  $P_{bbox}$ , and classification score  $S_{bbox}$ .  $P_{bbox}$  is filtered based on the defined threshold  $S_{threshold}$  for  $S_{bbox}$ . 2) The image  $I$  and a set of prompts  $P_{bbox}$  are input into SAM, to obtain prompt tokens  $T_{bbox}$  and masks  $M_{bbox}$ . 3) The  $M_{bbox}$  and the corresponding  $C_{bbox}$ , are randomly merged to obtain the final masks  $M_{semantic}$ . Considering the effectiveness of the YOLO series models, we choose the latest YOLOv8 as the object detector. The complete process is described as follows:

$$\begin{cases} C_{bbox}, P_{bbox} &= \begin{cases} \Phi_{det}(I) \\ S_{bbox} > S_{threshold} \end{cases} \\ F_I &= \Phi_{enc-i}(I) \\ T_{bbox} &= \Phi_{enc-p}(P_{bbox}) \\ M_{bbox} &= \Phi_{dec-m}(F_I, \text{Concat}(T_O, T_{bbox})) \\ M_{semantic} &= \text{Random}(C_{bbox}, M_{bbox}) \end{cases} \quad (2)$$

---

### Algorithm 1 Pseudocode in a Numpy-like style.

---

```
# img: an input image
# masks: The binary masks output by SAM.
# classes: The categories output by the detector.

# Pre-defined category fusion order.
order = ["ship", "land", "oil_spill", "look-alike"]

# Store the masks according to the 'order'.
h, w = img.shape[0], img.shape[1]
mask_list = []
zipped = zip(classes, masks)
order_key = lambda x: order.index(x[0])
orted_zipped = sorted(zipped, order_key)
for item in orted_zipped:
    c_mask = zeros((h, w, 1))
    class_id = item[0]
    mask = item[1]
    c_mask[mask] = class_id
    mask_list.append(c_mask)

# Fuse the masks.
mask_out = zeros((h, w, 1))
for mask in mask_list:
    mask_out[mask_out==0] = mask[mask_out==0]

return mask_out
```

---

### B. Ordered Mask Fusion module

The Ordered Mask Fusion (OMF) module is proposed to address pixel category conflicts encountered in mask fusion.

OMF operates based on a pre-defined mask order, where the ambiguous pixels are categorized based on the order, and the order is crucial to the OMF as detailed in Algorithm 1. For example, if the mask order is defined as 'ship, land, oil spill, look-alike', a pixel identified as both 'ship' and 'land' in the segmentation result will be classified as 'ship'.

### C. Adapted SAM

We adopt HQ-SAM [12] as the Adapted SAM because of its simplicity and training efficiency. The HQ-SAM was initially developed to enhance SAM's segmentation accuracy for intricate structures in natural images, while the HQ-SAM used in this study aims to improve SAM's ability to segment blurry boundaries in SAR imagery. HQ-SAM was constructed by introducing the fusion of HQ-Output Token and deep-shallow feature into SAM. Firstly, a learnable HQ-Output Token  $T_{HQ}$  is designed, which is input into SAM's mask decoder  $\Phi_{dec-m}$  together with the original prompts  $T_P$  and output token  $T_O$ . Unlike the original output token  $T_O$ , the HQ-Output Token  $T_{HQ}$  and its related Multi-layer Perceptron (MLP) layer are trained to predict high-quality segmentation masks. Secondly, by fusing the early feature  $F_{early}$  and late feature  $F_I$  of its image encoder, it uses both global semantic context and local fine-grained features. We refer to the combination of the HQ-Output Token, three-layer MLP, and a small feature fusion block as the Adapter module of HQ-SAM. The combination of the Adapter module and the original SAM decoder  $\Phi_{dec-m}$  forms a new decoder  $\Phi'_{dec-m}$ . During the training process, all the pre-trained SAM parameters are frozen, while only the Adapter module is updated. In summary, the SAM-OIL is composed of an object detector, HQ-SAM, and an OMF module, of which the whole process can be described as:

$$\left\{ \begin{array}{l} C_{bbox}, P_{bbox} = \begin{cases} \Phi_{det}(I) \\ S_{bbox} > S_{threshold} \end{cases} \\ F_{early}, F_I = \Phi_{enc-i}(I) \\ T_{bbox} = \Phi_{enc-p}(P_{bbox}) \\ T = \text{Concat}(T_{HQ}, T_O, T_{bbox}) \\ M_{bbox} = \Phi'_{dec-m}(F_{early}, F_I, T) \\ M_{semantic} = \Phi_{OMF}(C_{bbox}, M_{bbox}) \end{array} \right. \quad (3)$$

## III. EXPERIMENTS

### A. Experimental Setups

1) *Dataset*: The M4D dataset [4] was used in this study, which is created based on the geographical coordinates and timestamps provided by the CleanSeaNet service of the European Maritime Safety Agency. The dataset is composed of five categories: oil spill, look-alike, land, ship, and sea surface, and includes a total of 1,112 SAR images, each with a dimension of  $650 \times 1250$  pixels. The images were split into training and testing sets, where 1,002 images (90%) belong to training set and 110 images belong to testing set (10%). Fig.2 provides some SAR images from the M4D test dataset and their corresponding ground truths. The primary challenge in detecting oil spills from the M4D dataset lies in distinguishing between oil spills and look-alikes, both of which appear as

dark areas. Shorelines and ships are important contextual information [1], [3]. Therefore, it is necessary to detect land and ships to assist in identifying oil spills. The 'land' category is displayed as white areas on the SAR images, with distinct features. The 'ship' category appears as small white dots on the images, which are more difficulty to detect.

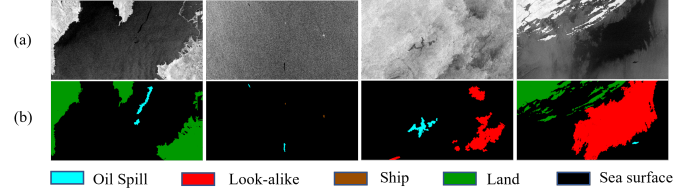


Fig. 2. Example images from the M4D test dataset: (a) SAR Images, (b) Ground Truth.

2) *Evaluation Metrics*: We adopt the Intersection over Union (IoU) and the mean Intersection over Union (mIoU) for the evaluation, which are commonly used in semantic segmentation. The IoU is used to assess the accuracy of each class, and the mIoU is used to evaluate the overall accuracy.

3) *Configuration Details*: All the experiments were conducted on two NVIDIA TITAN RTX GPUs (48G memory), with the operating system of Ubuntu 18.04.6 LTS. The object detector used was YOLOv8 within MMYOLO [11], configured with 1,000 training epochs and a batch size of 6, and other parameters remained the same as the default settings of MMYOLO. To maintain consistency with HQ-SAM's training scheme, the M4D dataset is refined by creating a binary mask for each object, without including any additional class information. All binary masks are used for training the HQ-SAM Adapter module. The training epoch is 120, the input image size is the original image size ( $650 \times 1250$ ), and the prompt type is bounding box. The ViT-H [9] model was employed as the image encoder for the SAM. The remaining parameters follow the HQ-SAM's default configuration.

### B. Comparative Experiments

Krestenitis *et al.* [4] proposed the M4D dataset and applied several classical semantic segmentation models (e.g., UNet, LinkNet, PSPNet, DeepLabv2, DeepLabv3+) for oil spill detection. We compare our proposed SAM-OIL with these classical models, as shown in Table I. From the results of Krestenitis *et al.* [4], the mIoU of the classical models ranged from 49.27% to 65.06%, where the performance of DeepLabv3+ was the best among the comparison models with the mIoU of 65.06%. By evaluating the results between SAM-OIL and the best classical models (i.e., DeepLabv3+), the proposed model is superior to the others, with a significant improvement in mIoU of 4.46% resulting in 69.52% mIoU. SAM-OIL also achieves the highest IoU in 'Look-alike' and 'Ship' categories. The performance of SAM-OIL is also outstanding when compared to the results of using YOLOv8-SAM only for all categories, particularly in 'oil spill' and 'look-alike', with increases of 9.76% and 7.45% respectively. For the 'oil spill', SAM-OIL presents a lower IoU than that of UNet by 2.19%, suggesting that SAM-OIL is slightly inferior

TABLE I  
QUANTITATIVE PERFORMANCE COMPARISON BETWEEN THE PROPOSED METHOD AND THE SEMANTIC SEGMENTATION METHODS ON THE M4D DATASET.

Methods	Sea Surface	Oil Spill	Look-alike	Ship	Land	mIoU
UNet	93.90	<b>53.79</b>	39.55	44.93	92.68	64.97
LinkNet	94.99	51.53	43.24	40.23	<b>93.97</b>	64.79
PSPNet	92.78	40.10	33.79	24.42	86.90	55.60
DeepLabv2	94.09	25.57	40.30	11.41	74.99	49.27
DeepLabv2 (msc)	95.39	49.53	49.28	31.26	88.65	62.83
DeepLabv3+	<b>96.43</b>	53.38	55.40	27.63	92.44	65.06
YOLOv8-SAM	94.34	41.84	48.15	52.48	87.65	64.89
SAM-OIL	96.05	51.60	<b>55.60</b>	<b>52.55</b>	91.81	<b>69.52</b>

\* All results are described using percentages (%). The accuracy of each category is evaluated using Intersection over Union (IoU). The best score is marked in bold. The accuracy of the semantic segmentation methods is sourced from [4].

TABLE II  
THE INFLUENCE OF OBJECT DETECTOR ON THE FINAL ACCURACY.

Methods	mIoU
YOLOv8-SAM	64.89
YOLOv8-SAM (gt_box)	77.09
SAM-OIL	69.52
SAM-OIL (gt_box)	<b>80.35</b>

TABLE III  
THE INFLUENCE OF OMF AND ADAPTER ON THE FINAL ACCURACY.

Methods	OMF	Adapter	mIoU
YOLOv8-SAM			64.89
YOLOv8-SAM + OMF	✓		65.82
YOLOv8-SAM + Adapter		✓	67.97
SAM-OIL (YOLOv8-SAM + OMF + Adapter)	✓	✓	<b>69.52</b>

TABLE IV  
THE INFLUENCE OF FUSION ORDERS OF OBJECT MASKS IN OMF ON THE FINAL ACCURACY.

Orders	Sea Surface	Oil Spill	Look-alike	Ship	Land	mIoU
Random	96.05	48.34	54.87	50.10	90.47	67.97
Look-alike, Oil Spill, Ship, Land	96.05	48.31	54.84	41.78	90.41	66.28
Look-alike, Oil Spill, Land, Ship	96.05	48.31	54.84	41.78	90.41	66.28
Look-alike, Land, Oil Spill, Ship	96.05	48.31	54.84	41.78	90.41	66.28
Ship, Oil Spill, Land, Look-alike	96.05	51.60	55.60	52.55	91.81	69.52
Ship, Land, Oil Spill, Look-alike	96.05	51.60	55.60	52.55	91.81	69.52
Land, Ship, Oil Spill, Look-alike	96.05	51.60	55.60	52.55	91.81	69.52

in detecting objects with fuzzy boundaries. For the category of 'ship', UNet is the best among the classic models, with the IoU of 44.93%. SAM-OIL achieves 52.55%, which is 7.62% higher than UNet. The result suggests that the object detector has a much better capability for detecting small objects when compared to semantic segmentation models.

### C. Ablation Study

We conducted extensive experiments to evaluate the impact of detector accuracy, detector classification scores, OMF, Adapter, and the category order of OMF on the final accuracy.

1) *Detector accuracy*: To assess the impact of detector performance on the final accuracy of oil spill detection, ground truth bounding boxes (gt\_box) are input into SAM and Adapted SAM respectively. As shown in Table II, YOLOv8-SAM (gt\_box) surpasses YOLOv8-SAM by 12.2%, and SAM-OIL (gt\_box) surpasses SAM-OIL by 10.83%. Table II demonstrates that the detector significantly impacts the final accuracy within the SAM-OIL framework.

2) *Detector classification scores*: The outputs of the detector include the coordinates of bounding boxes and the classification scores. The classification scores can be used to determine whether the bounding boxes should be ignored. As illustrated in Fig. 3, different classification score thresholds

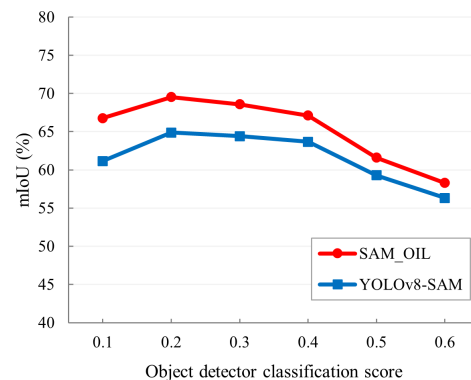


Fig. 3. The influence of object detector classification scores on the final accuracy.

can affect the final accuracy. When the classification score is 0.2, YOLOv8-SAM and SAM-OIL achieve the highest accuracy. Notably, the detection accuracy decreases significantly towards the increase of the classification score. A higher classification score tends to filter some accurate detected results, thereby inducing a lower accuracy.

3) *OMF*: As shown in Table III, YOLOv8-SAM+OMF surpasses the YOLOv8-SAM by 0.93%, and SAM-OIL surpasses



YOLOv8-SAM+Adapter by 1.55%. More importantly, OMF is a method without any training parameters. It should be noted that YOLOv8-SAM+OMF achieved mIoU of 65.82%, slightly surpassing DeepLabv3+'s 65.06% listed in Table I. Training the YOLOv8-SAM+OMF model requires only box-level annotated samples, which demonstrates the potential of SAM-based composite methods in reducing the workload of sample annotation.

4) *Adapter*: In Table III, YOLOv8-SAM+Adapter surpasses YOLOv8-SAM by 3.08%, and SAM-OIL surpasses YOLOv8-SAM+OMF by 3.7%. These results suggest that the Adapter can significantly improve the final accuracy.

5) *Order of OMF*: The masks outputted by SAM are categorized into four types: ship, land, oil spill, and look-alike. The arrangement of these four categories can be permuted in 24 ways, and considering random order, a total of 25 orders exist. In Table IV, the accuracy for random, worst, and best orders is presented. As indicated in the table, the accuracy difference between the best and worst orders is 3.24%, demonstrating that the order in OMF can significantly affect the final accuracy. The results suggest that higher priority should be given to the 'ship' and 'land' categories, while lower priority should be assigned to the 'look-alike' category. Since the 'ship' objects, typically small in satellite images, have classification accuracy that is more susceptible to influence, resulting in a lower mIoU. On the other hand, the 'land' class usually occupies a large portion of the image, with the exception of the 'sea surface', which serves as the background. The large 'land' objects lead to higher classification accuracy as they are easily detected. Therefore, prioritizing these two categories could minimize misclassifications. Additionally, since 'look-alike' may be adjacent to all other categories and tends to have lower accuracy, the results indicated that assigning it the lowest priority would enhance the overall performance.

#### D. Qualitative Analysis

Fig. 4 demonstrates the YOLOv8-SAM and SAM-OIL perform well in scenarios where there are elongated dark areas and small dark areas with simple surroundings, such as those without look-alikes (e.g., first column of Fig. 4). Benefiting from the integration of OMF and Adapter, the segmentation of objects with fuzzy boundaries using the SAM-OIL is more aligned with the ground truth, as illustrated in the second and third columns. Nevertheless, some small-sized look-alikes tend to be misclassified as oil spills by the SAM-OIL, highlighting the difficulty of determining oil spills based solely on SAR images.

#### IV. CONCLUSION

We propose a composite framework, SAM-OIL, which integrates YOLOv8 with the SAM, incorporating OMF and Adapter modules. To our best knowledge, this is the first time the SAM has been applied to oil spill detection. Compared to existing oil spill detection methods, SAM-OIL achieves the highest mIoU, demonstrating the significant potential of SAM-based composite framework in oil spill detection. Furthermore, the version of SAM-OIL without the Adapter module, namely

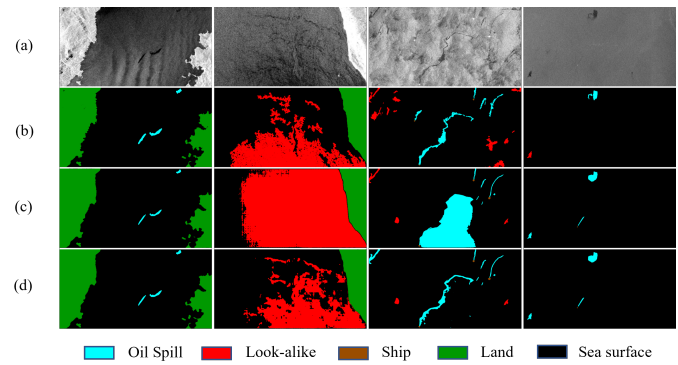


Fig. 4. Qualitative examples of YOLOv8-SAM and SAM-OIL. (a) SAR Images, (b) Ground Truth, (c) YOLOv8-SAM, (d) SAM-OIL.

YOLOv8-SAM+OMF, achieves accuracy comparable to existing oil spill detection methods. It indicates that the SAM-OIL framework can reduce the need for finely annotated samples. Our experimental results also suggest that the object detector has a large contribution on the final accuracy. Therefore, prioritizing the development of object detectors could further improve the detection performance in future.

#### REFERENCES

- [1] C. Brekke and A. H. Solberg, "Oil spill detection by satellite remote sensing," *Remote Sens. Environ.*, vol. 95, no. 1, pp. 1–13, 2005.
- [2] R. Al-Ruzouq, M. B. A. Gibril, A. Shanableh, A. Kais, O. Hamed, S. Al-Mansoori, and M. A. Khalil, "Sensors, features, and machine learning for oil spill detection and monitoring: A review," *Remote Sens.*, vol. 12, no. 20, p. 3338, 2020.
- [3] W. Alpers, B. Holt, and K. Zeng, "Oil spill detection by imaging radars: Challenges and pitfalls," *Remote Sens. Environ.*, vol. 201, pp. 133–147, 2017.
- [4] M. Krestenitis, G. Orfanidis, K. Ioannidis, K. Avgerinakis, S. Vrochidis, and I. Kompatsiaris, "Oil spill identification from satellite images using deep neural networks," *Remote Sens.*, vol. 11, no. 15, p. 1762, 2019.
- [5] C. Brekke and A. H. Solberg, "Classifiers and confidence estimation for oil spill detection in envisat asar images," *IEEE Geosci. Remote Sens. Lett.*, vol. 5, no. 1, pp. 65–69, 2008.
- [6] Q. Zhu, Y. Zhang, Z. Li, X. Yan, Q. Guan, Y. Zhong, L. Zhang, and D. Li, "Oil spill contextual and boundary-supervised detection network based on marine sar images," *IEEE Trans. Geosci. Remote Sens.*, vol. 60, pp. 1–10, 2021.
- [7] R. Hasimoto-Beltran, M. Canul-Ku, G. M. D. Méndez, F. J. Ocampo-Torres, and B. Esquivel-Trava, "Ocean oil spill detection from sar images based on multi-channel deep learning semantic segmentation," *Mar. Pollut. Bull.*, vol. 188, p. 114651, 2023.
- [8] X. Ma, J. Xu, P. Wu, and P. Kong, "Oil spill detection based on deep convolutional neural networks using polarimetric scattering information from sentinel-1 sar images," *IEEE Trans. Geosci. Remote Sens.*, vol. 60, pp. 1–13, 2021.
- [9] A. Kirillov, E. Mintun, N. Ravi, H. Mao, C. Rolland, L. Gustafson, T. Xiao, S. Whitehead, A. C. Berg, W.-Y. Lo, P. Dollar, and R. Girshick, "Segment anything," in *Proc. IEEE/CVF Int. Conf. Comput. Vis. (ICCV)*, October 2023, pp. 4015–4026.
- [10] K. Chen, C. Liu, H. Chen, H. Zhang, W. Li, Z. Zou, and Z. Shi, "Rsprompter: Learning to prompt for remote sensing instance segmentation based on visual foundation model," *arXiv:2306.16269*, 2023.
- [11] M. Contributors, "MMYOLO: OpenMMLab YOLO series toolbox and benchmark," <https://github.com/open-mmlab/mmyolo>, 2022.
- [12] L. Ke, M. Ye, M. Danelljan, Y. Liu, Y.-W. Tai, C.-K. Tang, and F. Yu, "Segment anything in high quality," in *NeurIPS*, 2023.